Ultrasonics 62 (2015) 46–49

Contents lists available at ScienceDirect

Ultrasonics

journal homepage: www.elsevier.com/locate/ultras

General properties of the acoustic plate modes at different temperatures

V.I. Anisimkin [a,*], I.V. Anisimkin [a,1], N.V. Voronova [b], Yu.V. Puchkov [b]

[a] Kotel'nikov Institute of Radio Engineering and Electronics, RAS, Moscow 125009, Russia
[b] Acoustoelectronics & Piezoceramic Elpa Corporation, Zelenograd, Moscow 124460, Russia

ARTICLE INFO

Article history:
Received 9 February 2015
Accepted 24 April 2015
Available online 11 May 2015

Keywords:
Acoustic plate mode
Piezoelectric plate
Temperature

ABSTRACT

Using acoustic plate modes with SH-polarization and quartz crystal with Euler angles 0°, 132.75°, 90°, as an example, general properties of the acoustic plate modes at different temperatures are studied theoretically and experimentally in the range from −40 to +80 °C. It is shown that in addition to well-known parameters responsible for temperature characteristics of acoustic waves the temperature coefficients of the acoustic plate modes depend on the mode order n, plate thickness h/λ, and expansion of the plate in direction of its thickness (h – thickness, λ – acoustic wavelength). These properties permit the mode sensitivity to be increased or decreased without replacing plate material and orientation.

1. Introduction

The value, sign, and temperature dependence of the temperature coefficient of delay (TCD) play an important role in almost all acoustic wave devices. Some of them (filters, resonators, delay lines) demand small TCD with weak temperature dependence. The others (temperature and thermal conductivity sensors) require high TCD and strong temperature dependence, on the contrary.

At present, the temperature properties of the surface (SAW) and bulk (BAW) acoustic waves are known for many solids, crystal cuts, and material combinations [1–4]. The same data for acoustic plate modes (APMs) are very restricted [5–7] though it is this type of the waves that is used for micro-wave filters, resonators, and sensors last time [8–11]. Since some APMs possess high velocities v [12], large coupling constants K^2 [12,13], and zero power flow angles Ψ [12] it could be expected that the temperature behaviour of the modes may also suggest some attractive properties.

The goal of the present paper is to study general properties of the acoustic plate modes at different temperatures and compare them with temperature properties of SAW and BAW in the same crystal.

2. Strategy

The temperature characteristics of SH-modes in quartz plates (Euler angles 0°, 132.75°, 90°) are calculated in the frame of linear elasticity using well-approved software [14] and temperature coefficients of elastic constants, density, and expansion up to 3rd order [15]. Temperature coefficients of piezoelectric and dielectric constants of only 1st order are used in calculations, but it seems to be quite reasonable restriction, because quartz is a weak piezoelectric material [3].

For SAW the temperature-delay coefficient is determined from the well-known expression $\mathrm{TCD} = (1/t)(d\tau/dt) = \alpha_{\parallel} - (1/v)(dv/dt)$ [1], where τ – delay, v – velocity, t – temperature, and $\alpha_{\parallel}$ – expansion of the crystal along propagation path (perpendicular to the X-axis in our case). On the contrary, for APMs, whose velocity v is changed with plate thickness h/λ, while h and λ are varied with temperature, expansion of the plate in direction of its thickness and the change in wavelength with temperature are additionally taken into account because of mode dispersion. Presenting dispersion as linear function $v = v(h/\lambda) + dv/d(h/\lambda) \times (h/\lambda)$, the APM temperature-delay characteristic is presented as:

$$\frac{\Delta\tau}{\tau} = \left[\alpha_{\mathrm{II}} - \frac{1}{v}\frac{dv}{dt}\right] \times \Delta t + \frac{1}{v}\frac{dv}{d(h/\lambda)} \times \left(\frac{h}{\lambda}\right) \times [\alpha_{\mathrm{II}} - \alpha_{\perp}] \times \Delta t \qquad (1)$$

Here, the 1st term is the same as that is for SAW. The 2nd term is a new contribution to $\Delta\tau/\tau$ depending on the slope of the dispersion curve $(1/v) \times dv/d(h/\lambda)$ at h/λ and the expansions of the crystal along propagation path $\alpha_{\parallel}$ and plate thickness $\alpha_{\perp}$. Δt is a change in crystal temperature with respect to 20 °C ($\Delta t = 0$ at $t = 20$ °C). The coefficients $\alpha_{\parallel}$ and $\alpha_{\perp}$ are calculated up to 3rd order using (i) expansions α_{11}, α_{22}, and α_{33} along crystallographic axis X, Y, and Z [15], (ii) 3D-shape of the quartz expansion (ellipsoid) [16], and (iii) particular orientation of the plate with respect to this ellipsoid. For plate orientation with Euler angles (0°, 132.75°, 90°) it takes:

* Corresponding author.
E-mail addresses: anis@cplire.ru (V.I. Anisimkin), vonavl@mail.ru (N.V. Voronova), ura@mail.ru (Y.V. Puchkov).
[1] Perished in terroristic attack.

http://dx.doi.org/10.1016/j.ultras.2015.04.010
0041-624X/

$$\alpha_{II}^2 = \frac{(\alpha_{11} \times \alpha_{33})^2}{0.54\alpha_{II}^2 + 0.46\alpha_{33}^2}; \quad \alpha_{\perp}^2 = \frac{(\alpha_{11} \times \alpha_{33})^2}{0.46\alpha_{11}^2 + 0.54\alpha_{33}^2} \tag{2}$$

For example, for mode $n = 0$ at $h/\lambda = 1.0$ and $t = 20$ °C($\Delta t = 0$): $\alpha_{\parallel} = 9.053$ ppm/°C, $\alpha_{\perp} = 9.453$ ppm/°C, $v = 4994.44$ m/s, $(1/v)dv/d(h/\lambda) = -10^{-3}$, and $\Delta v/v = \Delta\tau/\tau = 0$. For the same n and h/λ, but different $t = -40$ °C ($\Delta t = -60$ °C): $\alpha_{\parallel} = 8.826$ ppm/°C, $\alpha_{\perp} = 9.213$ ppm/°C, $v = 4980.27$ m/s, $(1/v)dv/d(h/\lambda) = -10^{-3}$, $\Delta v/v = -2837.15$ ppm, and $\Delta\tau/\tau = +2307.6$ ppm.

Experimental measurements performed in the paper are the same as described elsewhere [11]. In brief, they are based on quartz plates with different h/λ configured as APM delay lines. The lines are placed into a thermally insulated chamber (MLW U10, Sintz Friental, Medingen, Germany) allowing increase from 0 to 100 °C with accuracy ⩽0.1 °C. The temperature-delay characteristics $\Delta\tau/\tau$ are measured as phase-temperature characteristics $\Delta\phi/\phi_o$ because $\Delta\tau/\tau = \Delta\phi/\phi_o$, where ϕ_o is a total phase acquiring a mode from input to output transducer, $\Delta\phi$ is a change in phase produced by a change in temperature. The magnitude of ϕ_o is determined by geometry of the delay lines with high precision. The change $\Delta\phi$ is measured by a network analyzer (HP 8753E, Agilent Technologies, Santa Clara, CA) with accuracy ⩽0.1°. The order of the modes n is indentified from the phase velocities v_n determined as a product of a measured central frequency f_n and known wavelength λ that is equal to period of interdigital transducers.

At the beginning, both theoretical and experimental approaches of the paper are checked using well-approved SAW delay lines implemented on 3 semi-infinite quartz samples with different Euler angles (0°, 132.75°, 0°) (ST,X-cut), (0°, 130°, 0°), and (0°, 127°, 0°). The calculations for SAW are also compared with those from [15] where the same temperature coefficients of elastic constants, density, and expansion, but different software were used. After that, the same approaches are applied to APM samples supporting different plate modes. The modes with $n = 0$–7 and plates with $h/\lambda = 0.6$, 1.0, 1.2755 are studied in the range from $t = -40$ °C to +80 °C.

3. Results and discussion

Results of the paper are presented in Figs. 1–5. Fig. 1 demonstrates good agreement between calculated and measured results for 3 SAW samples. The calculations are also agreed with those from [15] accomplished for SAW in ST,X-quartz. Therefore, we consider our methods as approved for APMs measurements and calculations.

Dispersion of the modes studied in the paper is shown in Fig. 2. Velocity of the zero-order mode is almost constant for all thickness h/λ. Dispersion of the other modes is high for $h/\lambda \leqslant 1$ and low for $h/\lambda \geqslant 1$. For example, dispersion slope $(1/v_n)dv_n/d(h/\lambda)$ for the 7th mode is -1.62 for $h/\lambda = 0.6$ and -0.64 for $h/\lambda = 1.2755$.

In general, the more the slope, the larger contribution of the temperature-induced changes in plate thickness and relevant variations of the plate velocity to the temperature characteristics $\Delta\tau/\tau$ as follows from Eq. (1). Usually, these contributions (2nd term in (1)) are small compared with common value (1st term). However, in case they are comparable additional term corrects $\Delta\tau/\tau$ – characteristic. Example of this correction is shown in Fig. 3 for 2 modes with temperature coefficients closed to that of SAW in "temperature stable" ST,X-quartz (Euler angles 0°, 132.75°, 0°). It is seen that thanks to the 2nd term the minima of the curves are shifted on about 10 °C for both modes.

Temperature characteristics of SH-modes in quartz plates are presented on Figs. 4 and 5 together with the same characteristics for SH-BAW for comparison. The most important result followed from the figures is the dependence of the APM coefficients on the

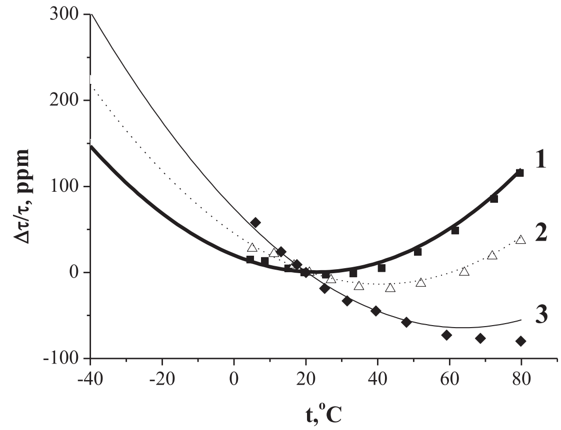

Fig. 1. Temperature-delay characteristics of the Rayleigh SAW in semi-infinite quartz samples. Solid lines: calculations. Points: experimental data. Euler angles: 1 – (0°, 132.75°, 0°) (ST,X-cut), 2 – (0°, 130°, 0°), 3 – (0°, 127°, 0°).

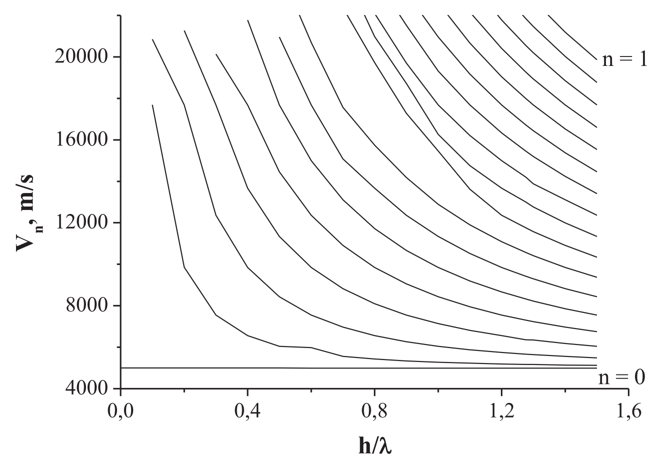

Fig. 2. Dispersion of SH-modes in quartz plate with Euler angles 0°, 132.75°°, 90° (ST,X + 90°-cut). The data are restricted by modes with non-zero coupling constants $K^2 \neq 0$.

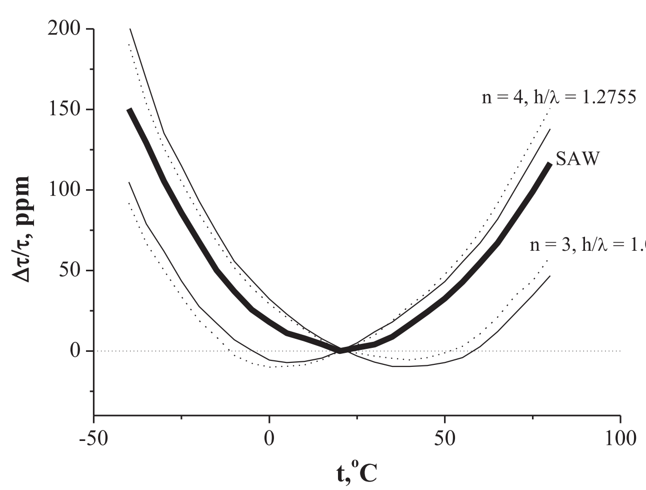

Fig. 3. Temperature characteristics of Rayleigh SAW in ST,X-quartz (bold) and SH-modes in ST,X + 90°-quartz (solid and dotted curves). Solid lines: the 2nd term of Eq. (1) is accounted. Dotted lines: the 2nd term of Eq. (1) is ignored.